Available online at www.sciencedirect.com
SCIENCE DIRECT
Microbes and Infection 8 (2006) 628–636
Microbes and Infection
www.elsevier.com/locate/micinf

Original article

Intragranulomatous necrosis in lungs of mice infected by aerosol with *Mycobacterium tuberculosis* is related to bacterial load rather than to any one cytokine or T cell type

Olga Gil [a], Evelyn Guirado [a], Sergi Gordillo [a], Jorge Díaz [a], Gustavo Tapia [b], Cristina Vilaplana [a], Aurelio Ariza [b], Vicenç Ausina [a], Pere-Joan Cardona [a,*]

[a] *Unitat de Tuberculosi Experimental, Department of Microbiology, Fundació Institut per a la Investigació en Ciències de la Salut Germans Trias i Pujol and Universitat Autònoma de Barcelona, Catalonia, Spain*
[b] *Department of Pathology, Fundació Institut per a la Investigació en Ciències de la Salut Germans Trias i Pujol and Universitat Autònoma de Barcelona, Catalonia, Spain*

Received 23 June 2005; accepted 30 August 2005
Available online 13 January 2006

Abstract

Low dose aerosol infection of C57BL/6 mice with a clinical strain of *Mycobacterium tuberculosis* (UTE 0335 R) induced intragranulomatous necrosis in pulmonary granulomas (INPG) at week 9 postinfection. Infection of different knockout (KO) mouse strains with UTE 0335 R induced INPG in all strains and established two histopathological patterns. The first pattern was seen in SCID mice and in mice with deleted α/β T receptor, TNF *R1*, IL-12, IFN-γ, or iNOS genes, and showed a massive INPG with a high granulomatous infiltration of the lung, a large and homogeneous eosinophilic necrosis full of acid-fast bacilli, with marked karyorrhexis, coarse basophilic necrosis, and surrounded by patches delimited by partially conserved alveolar septum full of PMNs. The second pattern was seen in mice with deleted IL-1 *R1*, IL-6, IL-10, CD4, CD8 or γ/δ T cell receptor genes, and showed more discrete lesions with predominant homogeneous eosinophilic necrosis with few bacilli and surrounded by a well-defined lymphocyte-based ring. Local expression of IFN-γ, iNOS, TNF and RANTES showed no significant differences between these mouse strains generating a discrete INPG. Mouse strains showing a massive INPG showed higher, lower or equal expression values compared to the control strain. In conclusion, the severity of the INPG pattern correlated with pulmonary CFU counts, irrespective of the genetic absence or the infection-induced levels of cytokine mediators.

Keywords: Intragranulomatous necrosis; Koch phenomenon; Shwartzman reaction; *Mycobacterium tuberculosis*; *Mycobacterium avium* complex; Cord factor; LPS; Tolerance; Mice

1. Introduction

Intragranulomatous necrosis (IN), defined as central necrosis that progresses to large areas of caseous consistency surrounded by macrophages and epithelioid cells also limited by a lymphocytic ring, is one of the most important characteristics of *Mycobacterium tuberculosis* lesions. This feature has classically been linked to a toxic reaction known as ''Koch's phenomenon'' [1]. The mechanisms associated with this reaction have not been clearly established to date. For a long time, delayed type hypersensitivity (DTH) (considered an independent form of cellular immunity) has been identified as the source of this necrosis by destroying poorly activated infected macrophages [1,2]. Other authors have found similarities between Koch's phenomenon and the classical Shwartzman reaction [3]. In this case, infected granulomas were considered to be ''prepared'' sites because of the presence of *M. tuberculosis*. The release of tumor necrosis factor (TNF) from macrophages activated and triggered in the lesion may cause tissue damage [4,5].

* Corresponding author. Unitat de Tuberculosi Experimental, Department of Microbiology, Hospital Universitari ''Germans Trias i Pujol'', Crta del Canyet s/n, 08916 Badalona, Catalonia, Spain. Tel.: +34 93 497 88 94; fax: +34 93 497 88 95.
E-mail address: pcardona@ns.hugtip.scs.es (P.-J. Cardona).

1286-4579/$ - see front matter © 2006 Elsevier SAS. All rights reserved.
doi:10.1016/j.micinf.2005.08.014

One of the main problems in the study of this phenomenon is that experimental models of *M. tuberculosis* infection do not induce IN in mice [6]. At the most, the largest lesions developed by mice (known as primary granulomas) show a macrophage-based center without epithelioid and Langhan's cells, surrounded by lymphocytes and by an outermost layer of foamy macrophages in the alveolar spaces [7]. Therefore, the immunological basis of the study of IN depends on experimental models using *Mycobacterium avium* strains able to induce such a necrosis [8–10]. These studies have revealed that the immunological mediators involved in the induction of protective immunity, such as $CD4^+$ T cells, IL-12p40 and IFN-γ, are essential for the induction of IN [8,9]. However, some controversy surrounds the role of high mycobacterial concentration or extensive granulomatous infiltration, since some authors do not relate them to necrosis [8] while others do [9]. Finally, the presence of TNF [10] does not seem to be involved in the development of IN in a model of *M. avium* infection in mice.

In this regard, our group previously worked in generating an experimental model of intragranulomatous necrosis in pulmonary granulomas (INPG) following the parallelism between Koch's and Shwartzman's reactions and previous experiments with experimental models in rabbits, which developed such a necrosis at the beginning of infection [11]. INPG was induced after intranasal inoculation of *Escherichia coli* lypopolysaccharide (LPS) in mice infected by aerosol with a low dose of *M. tuberculosis* at week 3 postinfection. This INPG was better structured at week 9 postinfection [12], when hematoxylin and eosin staining (H&E) revealed a fine homogeneous eosinophilic necrosis and a compact caseous consistency made of collagen (as demonstrated by trichrome staining) [13,14]. These lesions were similar to those found in human tuberculosis, although they lacked epithelioid and Langhan's cells and the intense fibrosis at the outermost layer [15,16]. Furthermore, the external ring of foamy macrophages still existed.

The finding of a *M. tuberculosis* (UTE 0335 R) clinical strain that induced necrosis in wild type C57BL/6 mice [17,18] and reproduced the same pattern previously found with our experimental model encouraged us to study the immunological basis of this phenomenon. Hence, we infected different KO mice lacking essential cytokines and cells to induce protective immunity. Interestingly, our data did not reproduce previous information based on *M. avium* infections. Nevertheless, the expression of cytokines and the presence of cells involved in host protection are not essential for the induction of INPG. Furthermore, in our study we observed two patterns of INPG: one massive and one discrete. A massive INPG was associated with high bacillary load and extensive granulomatous infiltration with local expression of IFN-γ, iNOS and TNF higher, lower than or equal to that found with the wild type C57BL/6 control strain. Discrete INPG was found in mouse strains presenting the same values as the control strain.

2. Materials and methods

2.1. Mice

C57BL/6, C57BL/6 IL-10 knockout (KO) and CB17/Icr-SCID specific pathogen free (*spf*) 6–8-week-old female mice were obtained from Charles River Laboratories (St Germain sur l'Abresle, France). The following *spf*, 6–8-week old, female KO mouse strains with a C57BL/6 background were purchased from The Jackson Laboratory (Bar Harbor, ME, USA): αβ TCR-KO, γδ TCR-KO, CD4-KO, CD8-KO, IFNγ-KO, TNF *R1* KO, IL-1 *R1* KO, IL-6-KO, IL-10-KO and IL-12p40 KO. iNOS-KO mice were kindly donated by Dr. Irene García-Gabay from the Department of Pathology, University of Geneva, Switzerland. They were shipped in suitable travel conditions, with the corresponding certificate of health and origin. All the animals were kept under controlled conditions in a P3 high security facility with sterile food and water ad libitum.

2.2. Bacteria and infection

M. tuberculosis strain UTE 0335 R induced pulmonary TB in a 32-year-old HIV^- male (alcoholism was the only risk factor). The minimal inhibitory concentration (MIC) for isoniazid was 8 μg/mL and a mutation in *katG* (AGC_ACC) was detected; no mutations were detected in *inhA* [17,18]. UTE 0335 R was grown in Proskauer Beck medium containing 0.01% Tween 80 to mid-log phase and stored at −70 °C in 2 mL aliquots. Mice were placed in the exposure chamber of an airborne infection apparatus (Glas-col Inc., Terre Haute, IN, USA). The nebulizer compartment was filled with 7 ml of a *M. tuberculosis* suspension at a previously calculated concentration to provide an approximate uptake of 20 viable bacilli within the lungs. Four mice were used for every time point in every experimental group. The number of viable bacteria in the left lung and spleen homogenates was measured at weeks 9 and 18 by plating serial dilutions on nutrient Middlebrook 7H11 agar (Biomedics s.l., Madrid, Spain) and counting bacterial colony formation after 21 days of incubation at 37 °C. Special care was taken not to include hilar lymph nodes at the time of removal of the left lung in order to not artificially increase the CFU value. Lungs were immediately extracted after euthanasia by means of a halothane overdose (Zeneca Farma, Pontevedra, Spain).

2.3. Animal health

Mice were weighed once a week. They were supervised every day under a protocol paying attention to weight loss, apparent good health (bristled hair and wounded skin) and behaviour (signs of aggressiveness or isolation). Animals were euthanized with halothane (Fluothane, Zeneca Farma) overdose so as to avoid suffering. Sentinel animals were used to check *spf* conditions in the facility. Tests for 25 known mouse pathogens were all negative. All experimental proceedings were approved and supervised by the Animal Care Committee of "Germans Trias i Pujol" University Hospital in agreement with the European Union Laws for protection of experimental animals.

2.4. mRNA quantification

The procedures have been described elsewhere [18]. In short, total RNA from the middle right lobe was extracted with a commercial phenol–chloroform method, RNAzol

(Cinna/Biotecx, Friendswood, TX, USA). After DNase treatment with DNA-free kit (Ambion, Woodward Austin, USA), a denaturing agarose gel was used to assess the stability of RNA. RNA (5 μg) was reverse transcribed using a Superscript RT kit (Gibco BRL, Grand Island, NY, USA) following the manufacturer's recommendations for obtaining cDNA. The quantitative analysis for IFN-γ, RANTES, iNOS, IL-4, IL-10 and TNF was performed using a LightCycler™ System (Roche Biochemicals, Idaho Falls, ID, USA). A real-time PCR was carried out in glass capillaries to a final volume of 10 μL in the presence of 1 μL of 10× reaction buffer (*Taq* polymerase, dNTPs, $MgCl_2$, SYBRGreen, Roche Biochemicals), and 1 μL of cDNA (or water as negative control, which was always included), $MgCl_2$ to a final concentration of 2–5 mM and primers to a final concentration of 0.5 μM were also added. A single peak was obtained for each PCR product by melting curve analysis, and only one band of the estimated size was observed on the agarose gel. Hypoxanthine guanine phosphoribosyl transferase (HPRT) mRNA expression was analyzed in all target samples to normalize for efficiency in cDNA synthesis and RNA loading. A ratio based on HPRT mRNA expression was obtained for each sample.

2.5. Histology and morphometry

Procedures have been described in previous works [18]. Briefly, two right lung lobes from each mouse were fixed in buffered formalin and subsequently embedded in paraffin. All samples were stained with hematoxylin–eosin, Masson trichrome and Ziehl–Neelsen. For histometry, 5 μm-thick sections from each specimen were stained with hematoxylin–eosin and photographed at 6× using a Stereoscopic Zoom SMZ800 microscope (Nikon, Tokyo, Japan) and a Coolpix 990 digital camera (Nikon). Sections of eight lung lobes were studied in each case. Several suitable software programs were used to determine the area of each single lesion and the total tissue area on photomicrographs, using appropriate software: Scion Image (Scion Corporation, Frederick, Maryland, USA) and Photoshop 5.0 (Adobe Systems Incorporated, San José, California, USA). Sections were blindly evaluated in order to get more objective measurements.

2.6. Statistical analysis

Sigma Stat (Jandel Scientific Software, San Rafael, California, USA) was used to compare means of values, and the differences between all values compared to control (CT) were determined using multiple comparisons versus control group (Dunnett's method). Differences were significant when marked with * for $p < 0.05$.

3. Results

3.1. Histopathological analysis reveals two patterns of INPG: massive and discrete

Fig. 1 shows the histology of the granulomas induced in all mouse strains infected with *M. tuberculosis* UTE 0335 R.

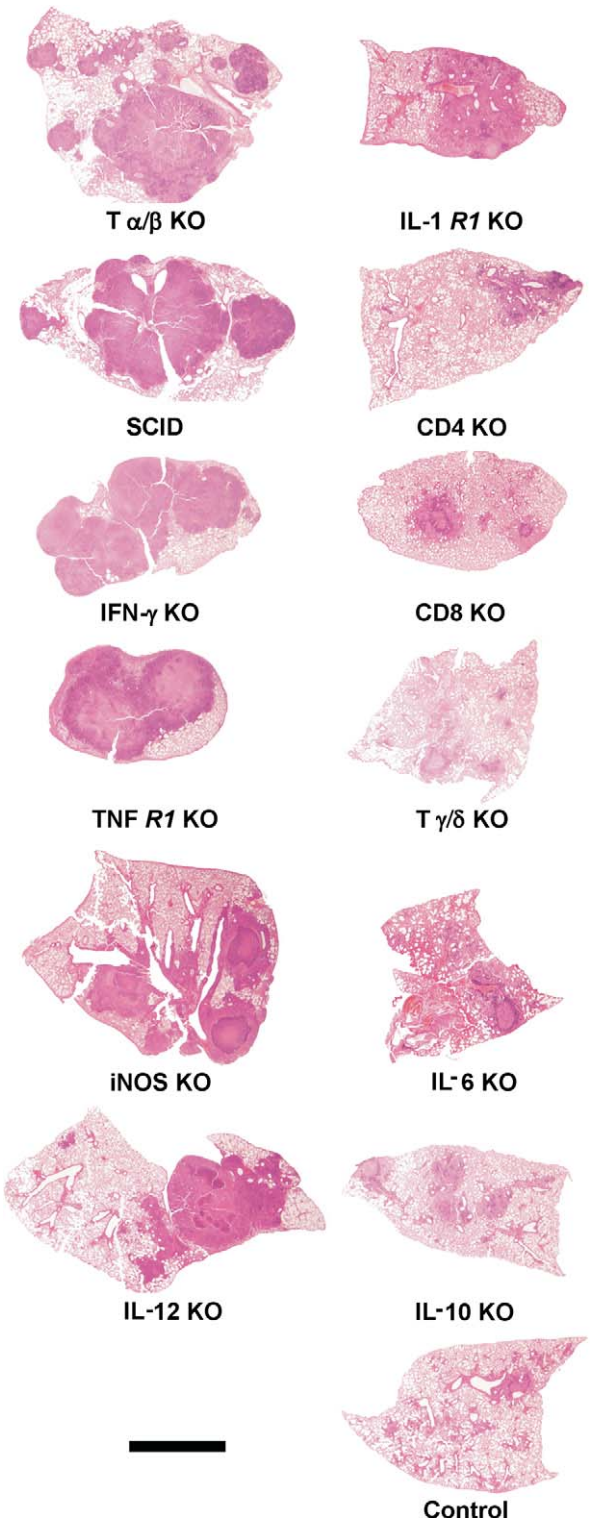

Fig. 1. Histology of representative hematoxylin–eosin stained sections from entire pulmonary lobes at 4 weeks (SCID mice and mice with deleted Tα/β receptor, IFN-γ, and TNF *R1* genes), 5 weeks (iNOS deleted gene) and 9 weeks postinfection (the remaining mouse strains) at low-power magnification (10×). Pictures from mouse strains with a massive INPG pattern are shown in the left column, while those displaying a discrete pattern are in the right column. The bar represents 3 mm.

These low-power pictures of sections stained with H&E present the two major patterns obtained. The left column shows representative sections from Tα/β, IFN-γ, TNF *R1* KO and SCID mouse strains developing a massive pattern of INPG. These microphotographs were taken at week 4 postinfection, when the animals had to be sacrificed. iNOS and IL-12 KO strains are also included in this group, although the samples were obtained at 5 and 9 weeks postinfection, respectively, because the condition of the mice made it possible to keep them alive until then. The right column shows the mouse strains that developed a discrete INPG. IL-1 R1, CD4, CD8, Tγ/δ, IL-6, and IL-10 KO mice, as well as wild type C57BL/6 mice (control group), were sacrificed at week 9 postinfection, the time point previously chosen to evaluate INPG. All these strains except IL-1 *R1* KO were still alive at week 18 postinfection (the end of the experiment) and maintained their INPG pattern (data not shown).

The high-power amplification pictures shown in Fig. 2 allowed a more detailed analysis of the patterns. The discrete pattern from IL-6 KO mice (Fig. 2A–C) consisted of small lesions with predominant homogeneous eosinophilic necrosis, together with very few spots showing karyorrhectic debris and clumps with mostly dead neutrophils (PMN). Necrotic tissue was well delimited by macrophages and a thick mantle of lymphocytes. Masson trichrome staining revealed the presence of some small homogeneous zones with a high collagen content. Intact macrophages were found inside the necrotic mass. Few acid-fast bacilli were detected, and these were usually present in small spots with karyorrhexis and coarse basophilic necrosis.

The massive pattern (Fig. 2D–F) was characterized by the presence of a large, fine and homogeneous eosinophilic necrosis with wide areas showing marked karyorrhexis and other areas with coarse basophilic necrosis related to the presence of PMN, mostly degenerated. The border of these granulomas was marked by patches delimited by partially conserved alveolar septum full of PMNs and massive karyorrhexis (e.g., as in acute pneumonia). Very few lymphocytes were found. Masson trichrome staining revealed the presence of collagen. High numbers of acid-fast bacilli were found in all the necrotic tissue. Remarkably, abscesses were found in iNOS-KO mice.

3.2. Massive INPG pattern is linked both to high bacillary load and extensive granulomatous pulmonary infiltration

Bacillary concentrations in the lungs were clearly different in groups with massive INPG and groups developing discrete INPG (Fig. 3). Mean values were significantly higher (usually more than 3 $\log_{10}$ higher) in groups with massive INPG compared to control mice, whereas no significant differences were found between control mice and groups with discrete INPG. However, there was one exception, IL-1 *R1* KO mice, which also harbored a high bacillary concentration but showed a discrete INPG pattern. This strain may be considered to be a borderline group, as the difference between mean concentrations was around 1.5 $\log_{10}$. The same relationship was established for the values obtained from the spleen. In this case, the borderline group might be even broader and may also include TNF *R1* and CD8-KO mice, which have a difference of 2 $\log_{10}$ compared to the controls. In this case, data reflect an increase or decrease of the hematogenous dissemination contention, depending on the group in which every strain was formerly classified.

The same standard was found for granulomatous infiltration (Fig. 4). The difference between strains with either INPG pattern was enormous. The infiltration percentages were 39–63% for massive INPG and 5–32% for discrete INPG. This is really relevant, since previous data from highly virulent *M. tuberculosis* strains in wild type C57BL/6 showed an infiltration rate of

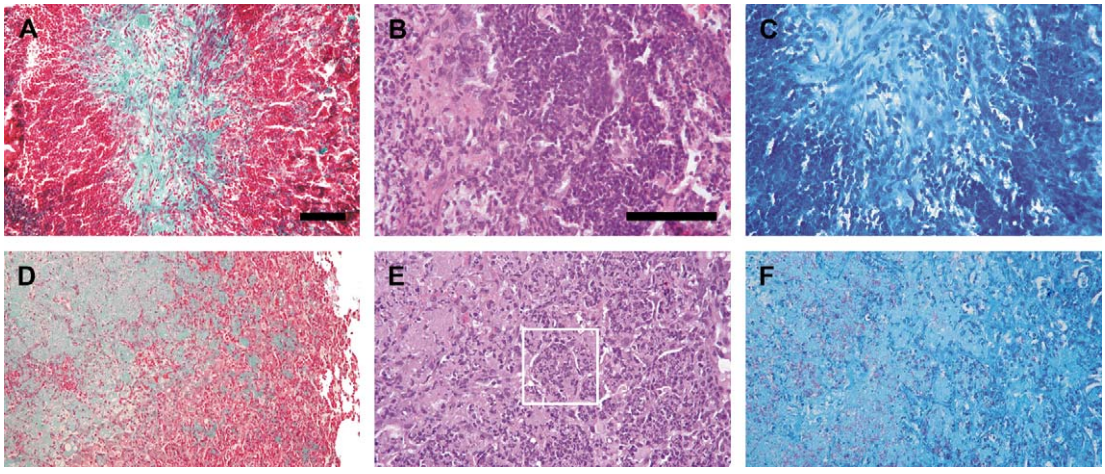

Fig. 2. Histopathological INPG analysis of two mouse strains representative of discrete (A–C) and massive (D–F) patterns from mice with deleted IL-6 and TNF *R1* genes, respectively. A and D display the total area of both granulomas with Masson trichrome stain (original amplification × 200) showing the collagen-rich central necrotic area (in green). These images are amplified in the pictures, B and C for A, and E and F for D. In B, H&E staining reveals a higher cellularity and a more structured granuloma, with a thick peripheral mantle of lymphocytes, whereas in E there is massive karyorrhexis and the edge is marked by patches delimited by partially conserved alveolar septum full of PMNs (marked in a white square). Very few lymphocytes are found in this lesion. C and F are stained with Ziehl–Neelsen. F shows a massive and generalized presence of these bacilli in the necrotic area. Bars represent 200 μm.

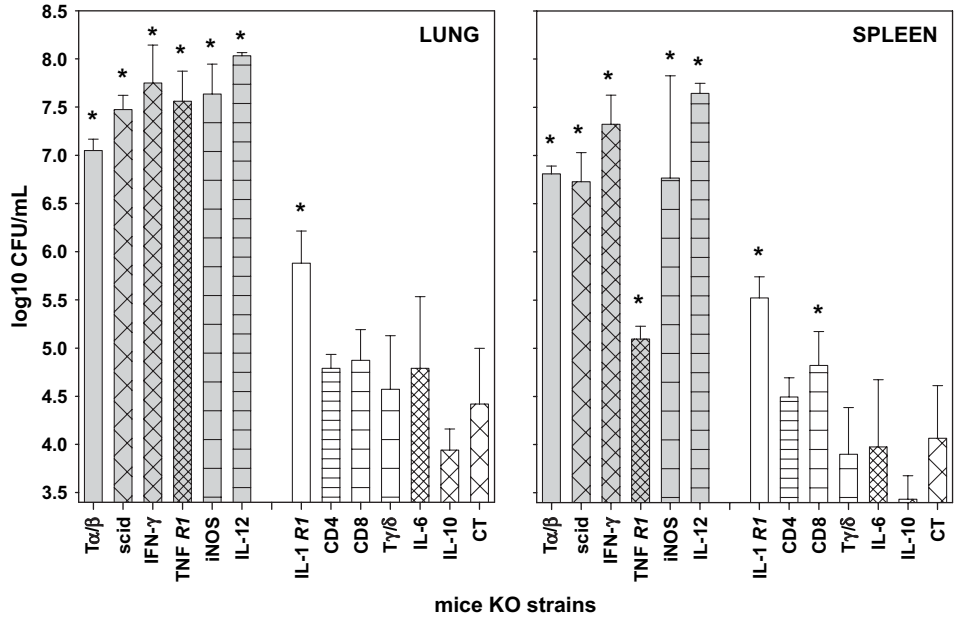

Fig. 3. Bacillary concentration in the lungs and spleen at 4 weeks (SCID mice and mice with deleted Tα/β receptor, IFN-γ, and TNF *R1* genes), 5 weeks (mice with deleted iNOS gene) and 9 weeks postinfection (the remaining mouse strains). Mouse strains presenting a massive INPG pattern are grouped at the left side of the graphics and are represented by gray bars. Mouse strains presenting a discrete pattern are grouped at the right side with white bars. Values represent the mean and standard deviation from four mice. Multiple comparisons versus control group (Dunnett's method) are used to determine the differences for all values compared to control (CT). Significant differences are marked with * for $p < 0.05$.

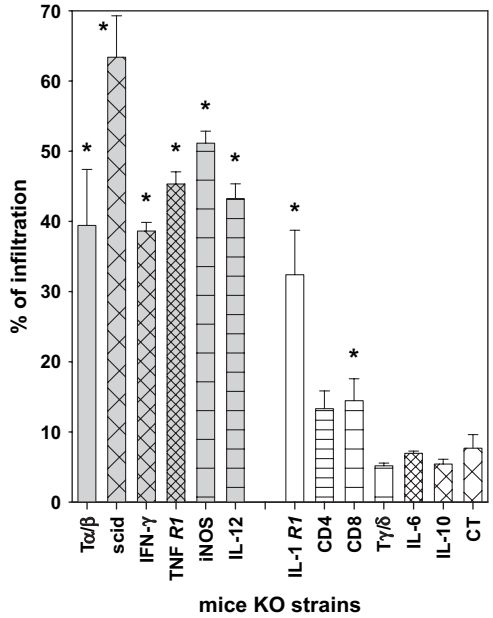

Fig. 4. Percentage of pulmonary infiltration by granulomatous lesions at 4 weeks (SCID mice and mice with deleted Tα/β receptor, IFN-γ, and TNF *R1* genes), 5 weeks (mice with deleted iNOS gene) and 9 weeks postinfection (the remaining mouse strains). Mouse strains presenting a massive INPG pattern are grouped at the left side of the graphics and represented by gray bars. Mouse strains presenting a discrete pattern are grouped at the right side with white bars. The percentage of pulmonary infiltration was obtained after dividing the area of granulomatous infiltration by the total area of the lobes multiplied by 100. Values represent the mean and standard deviation from four mice. Multiple comparisons versus control group (Dunnett's method) are used to determine the differences for all values compared to control (CT). Significant differences are marked with * for $p < 0.05$.

35% at week 22 postinfection [7,8]. Again, IL-1 *R1* KO mice showed a special characteristic consisting of a high granulomatous infiltration rate despite presenting a diffuse pattern, probably caused by extensive pulmonary dissemination.

3.3. Mice KO strains with a discrete INPG pattern have local pulmonary mRNA expression of IFN-γ, TNF R1, iNOS and RANTES similar to wild type control mice

The study of local mRNA expression of TNF, IFN-γ, RANTES and iNOS, all of which are related to host protection against *M. tuberculosis* infection [18], reveals a homogeneous profile in strains displaying a discrete pattern of INPG. Mean values were not significantly different compared to control strains (Fig. 5), save for iNOS expression in IL-1 *R1* KO, which probably reflects a massive diffuse infiltration and greater levels of foamy macrophages [18]. Furthermore, mouse strains showing a massive INPG pattern showed higher, lower or even equivalent values compared to controls, thus suggesting the low relevance of these parameters in the induction of massive INPG.

No expression of IL-4 and IL-10 was detected in any mouse strain (data not shown).

4. Discussion

The origin of IN in tuberculosis is still controversial. Robert Koch described it experimentally in guinea pigs already ill with tuberculosis and subcutaneously re-inoculated with living or killed bacilli [1]. IN is basic in the immunopathology of

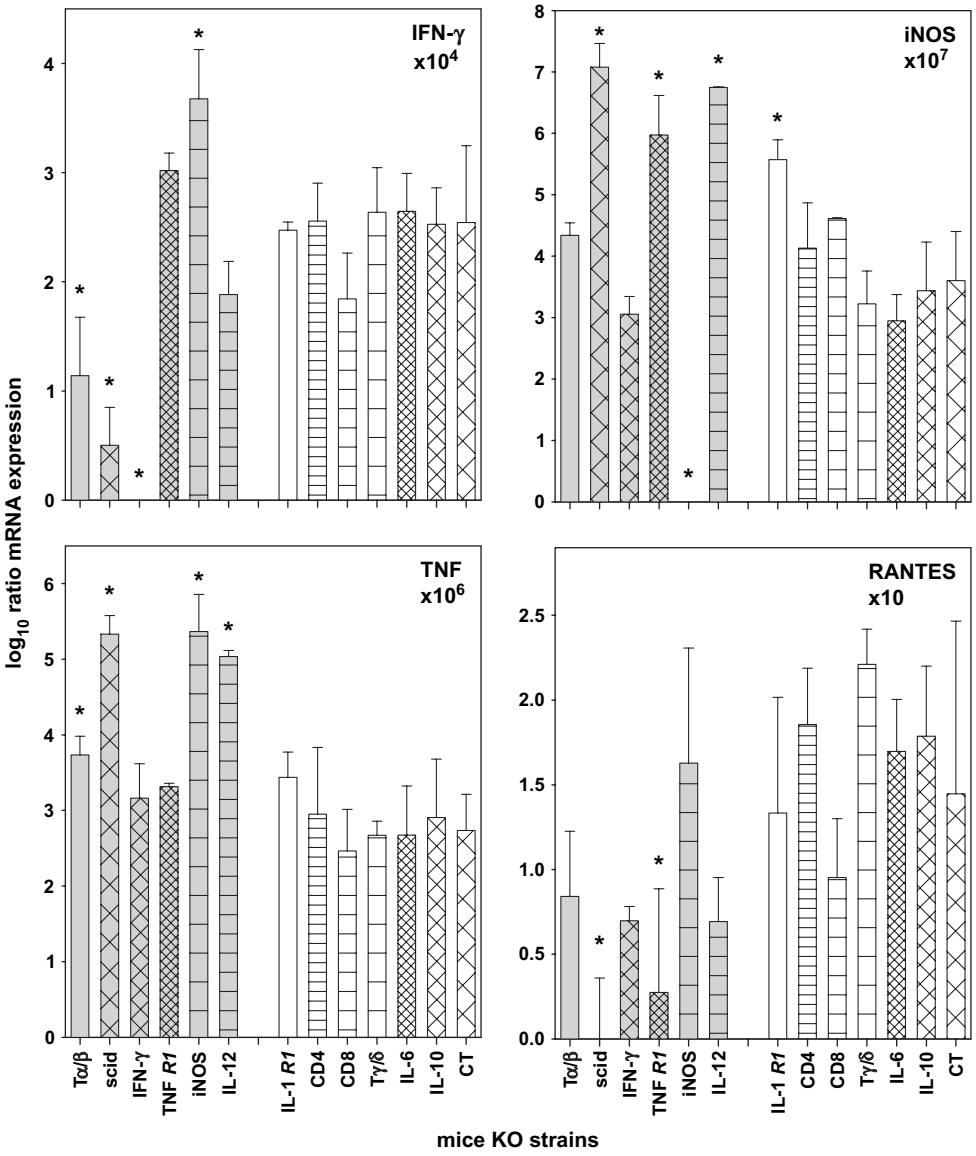

Fig. 5. Local pulmonary mRNA expression of IFN-γ, iNOS, TNF and RANTES, expressed as $\log_{10}$ of the ratio obtained after dividing each by the expression of HPRT in each sample and multiplying it by a factor (ranging from 10 to 10^7) at 4 weeks (SCID mice and mice with deleted Tα/β receptor, IFN-γ, and TNF *R1* genes), 5 weeks (mice with deleted iNOS gene) and 9 weeks postinfection (the remaining mouse strains). Mouse strains presenting a massive INPG pattern are grouped at the left of the graphics and represented by gray bars. Mouse strains presenting a discrete pattern are grouped at the right side with white bars. Values represent the mean and standard deviation from four mice. Multiple comparisons versus control group (Dunnett's method) are used to determine the differences for all values compared to control (CT). Significant differences are marked with * for $p < 0.05$.

tuberculosis, not only because it is the origin of both tissue destruction and extracellular bacillary population as well as the source of latent bacilli [19], but also because its progression and liquefaction is the origin of cavitation, the most common form of tuberculosis, and thus the primary source of infecting bacilli [15,16].

Therefore, IN is crucial in the study of tuberculosis but it is the least understood of all events. For a long time, IN has been linked to DTH (considered as an independent form of cellular immunity), essentially as a mechanism to destroy macrophages that are poorly activated by cellular-mediated immunity and thus harbor living bacilli [1,2] or as a cytotoxic activity mostly mediated by $CD8^+$ cells [20]. Another perspective was given by suggesting that the origin of IN was a local type of Shwartzman reaction [5] and that TNF plays a key role in the development of IN based on the evidence obtained using an experimental model of skin lesions in foot pads [4], which also showed that a Th2 environment would favor such a necrosis [21].

One of the main problems in the study of IN is that although most mammalian species develop it [22], mice do not [6]. Hence, we hypothesized that mice may be quite tolerant to the presence of *M. tuberculosis*. This is supported by the relative ease with which the bacilli may leave the granuloma harbored by macrophages [7] or by the fact that induction of DTH in mice requires a higher dose of PPD compared to humans or guinea pigs [23,24] (100 and 10 times higher, respectively). This tolerance may be the result of the small size of mice compared to other animals. A simple look at a cavitated

pulmonary lesion, which usually weighs more than 100 g, explains why mice are unable to develop them (as their total body weight is around 30 g). Maybe for this reason, although infected granulomas in mice are also ''prepared'' zones, not enough TNF is secreted by activated macrophages in order to induce necrosis in these small animals. Thus, we decided to inoculate the mice with intranasal LPS at the beginning of infection (week 3 postinoculation), which is when necrosis increased at least in the rabbit experimental model [11]. This was the origin of the ''humanized'' experimental model of tuberculosis [12], as a well-defined intragranulomatous necrosis in pulmonary granulomas (INPG) with homogeneous eosinophilic necrosis and caseous consistence was obtained at week 9 postinfection. Unfortunately, this model was somewhat artificial, as LPS inoculation introduced a highly significant factor that would lead to erroneous conclusions when searching for the immunological basis of IN.

Meanwhile, the appearance of *M. avium* strains able to induce IN [8,9] in the experimental model induced by intravenous or aerosol inoculation gave new insight into the issue. *M. avium-intracellulare* complex (MAC) infection in humans usually causes a disseminated disease but may also cause cavitary lung lesions [25,26], although histologically the lungs show granulomatous inflammation with a lower tendency to necrotize than with *M. tuberculosis* [27]. However, in this case the necrotic areas are filled with inflammatory cells and nuclear debris rather than the acellular areas of caseation found in tuberculosis [28]. Furthermore, the incidence of MAC infection has increased due to an increase in HIV infection and AIDS, and patients rarely have $CD4^+$ cell counts higher than 100/mm^3. Histologically, MAC infection in these patients can usually be distinguished from disseminated tuberculosis by the presence of poorly formed granuloma, the lack of necrosis, and the presence of macrophages heavily infested with bacilli [25,27–29]. In fact, cavitary lesions are uncommon while developing focal pulmonary disease (<5%) [25]. Taking into account these circumstances, the findings previously obtained with the *M. avium* experimental model [8,9] are quite consistent with the pathological data obtained from humans, thus suggesting a paramount role of $CD4^+$ cells and IFN-γ and IL-12p40 cytokines.

These results are totally different from those we have obtained, since all KO mouse strains tested developed INPG. Besides, in our work, the bacterial load in the parenchyma was a relevant factor; this is also the case in the model of infection induced by intravenous infection [9], but not in the aerosol model with *M. avium* [8]. In the latter case, concentration levels increased to up to 10 $\log_{10}$, which is suggestive of macrophages heavily infested with bacilli, and did not cause the death of the animal or induce necrosis. In our model, a bacillary concentration a thousand times higher than the control (i.e., 7.5 $\log_{10}$) correlated with the induction of a massive INPG. The remaining mice also generated INPG, although discrete. Hence, there must be something related to the antigenic nature of both mycobacterial species that induces *M. tuberculosis* to trigger an intense inflammatory response that is more reactive than *M. avium*. In this case, the parallelism with the Shwartzman reaction may be linked to the relative scarcity or low activity of LPS-like molecules from *M. avium* cell wall compared to *M. tuberculosis*. The presence of molecules like trehalose dimycolate (cord factor) may play a crucial role, as differences in its composition have already been detected between these species [30–33].

Interestingly, the presence of TNF was not crucial for the induction of IN in the *M. avium* model [10]. This work emphasized the role of IFN-γ in the generation of IN. This fact is not in disagreement with the theory that Koch's phenomenon may be associated with some kind of Shwartzman reaction. Evidence demonstrates that IL-12 and IFN-γ may act as LPS for ''preparing'' zones to induce this phenomenon, and IL-1 or even IFN-γ may act as a ''challenge'' to induce the reaction [34]. The fact that different cytokines may act in diverse ways to reproduce the Shwartzman reaction could explain why INPG is still induced in our model despite the absence of TNF *R1*. In fact, we have observed that the INPG pattern is massive in the TNF *R1* KO strain. Again, the answer might be found in the high bacillary load reached in the lungs. Recently, TB models in guinea pigs have revealed the importance of the accumulation of eosinophiles at the beginning of the infection, and its potential as a source of IN [35,36]. This observation also supports the idea that IN does not need the presence of specific immunity to be triggered. On the other hand, we could only demonstrate the presence of neutrophils in the lesions of all the mice strains used (data not shown), indicating that this mechanism does not explain the origin of IN in our study.

The presence of this massive pattern in iNOS-KO mice again reveals the key role of NO in the control of bacillary concentration, as previously described elsewhere [37]. The timing of NO production is also important. The expression of iNOS has been associated with protection and control of the infection at the beginning of the process, but it may also be linked to an antibacterial activity at later stages, at the chronic phase [38], when it is induced in foamy macrophages and may lead to local immunosuppression [18,38]. In fact, the biological action of NO is quite controversial, as it has also been associated with the induction of an increased or decreased inflammatory response [38,39].

Tγ/δ lymphocytes have been linked to the control of inflammatory response in murine models of tuberculosis [40]. Our data reveal that these cells do not affect the induction of INPG; neither does the absence of IL-10, a strong anti-inflammatory cytokine [41] that acts as a counter-balance to the proinflammatory activity of TNF. Finally, the lack of IL-6 neither affected the induction of INPG nor triggered a massive pattern. This cytokine is associated with stimulation of Th1 immunity at the beginning of infection, but does not affect the bacillary load as much as other Th1-related cytokines [42]. Interestingly, the presence or absence of $CD8^+$ cells, which may contribute to cytotoxicity in *M. tuberculosis* infection and thus be a key cell population in the induction of necrosis [20], was not significant either for the development of INPG.

In conclusion, intragranulomatous necrosis in pulmonary granulomas (INPG) in an experimental model of murine tuberculosis induced by aerosol is not related to the levels of individual cytokines. A high bacillary concentration in the

lungs increases the magnitude of INPG, thus indicating that the composition of the bacilli may be involved in the induction of some kind of nonspecific Shwartzman-like reaction. The complexity of this reaction and the fact that it may be elicited by different cytokines explains why this same reaction may be induced even when crucial cytokines such as IFN-γ are missing, and thus none of these are indispensable for generating INPG.

Acknowledgements

This work has been funded by Grants FIS 01/0644, 01/3104 and 03/0757. We thank Ms Marga Ortiz, from the Center for Animal Experimentation, and the technicians at the Pathology Department, Hospital Universitari Germans Trias i Pujol, for their technical support, and Mrs. Deborah Cullell for her excellent work in English reviewing.

References

[1] G.H. Bothamley, J.M. Grange, The Koch phenomenon and delayed hypersensitivity: 1891–1991, Tubercle 72 (1991) 7–11.
[2] A.M. Dannenberg Jr., Delayed-type hypersensitivity and cell-mediated immunity in the pathogenesis of tuberculosis, Immunol. Today 12 (1991) 228–233.
[3] G. Shwartzman, Phenomenon of Local Tissue Reactivity and its Immunological, Pathological and Clinical Significance, Paul B. Hober, New York, 1937.
[4] R. al Attiyah, H. Rosen, G.A. Rook, A model for the investigation of factors influencing haemorrhagic necrosis mediated by tumour necrosis factor in tissue sites primed with mycobacterial antigen preparations, Clin. Exp. Immunol. 88 (1992) 537–542.
[5] G.A. Rook, R. al Attiyah, Cytokines and the Koch phenomenon, Tubercle 72 (1991) 13–20.
[6] M.J. Lefford, Diseases in mice and rats, in: G.P. Kubica, L.G. Wayne (Eds.), The Mycobacteria: A Source Book, Marcel Dekker Inc., New York, 1984, pp. 947–977.
[7] P.J. Cardona, R. Llatjos, S. Gordillo, J. Diaz, I. Ojanguren, A. Ariza, V. Ausina, Evolution of granulomas in lungs of mice infected aerogenically with *Mycobacterium tuberculosis*, Scand. J. Immunol. 52 (2000) 156–163.
[8] S. Ehlers, J. Benini, H.D. Held, C. Roeck, G. Alber, S. Uhlig, Alphabeta T cell receptor-positive cells and interferon-gamma, but not inducible nitric oxide synthase, are critical for granuloma necrosis in a mouse model of mycobacteria-induced pulmonary immunopathology, J. Exp. Med. 194 (2001) 1847–1859.
[9] M. Florido, A.M. Cooper, R. Appelberg, Immunological basis of the development of necrotic lesions following *Mycobacterium avium* infection, Immunology 106 (2002) 590–601.
[10] M. Florido, R. Appelberg, Granuloma necrosis during *Mycobacterium avium* infection does not require tumor necrosis factor, Infect. Immun. 72 (2004) 6139–6141.
[11] M.B. Lurie, The correlation between the histological changes and the fate of living tubercle bacilli in the organs of tuberculous rabbits, J. Exp. Med. 55 (1932) 31–58.
[12] P.J. Cardona, R. Llatjos, S. Gordillo, J. Diaz, B. Vinado, A. Ariza, V. Ausina, Towards a 'human-like' model of tuberculosis: intranasal inoculation of LPS induces intragranulomatous lung necrosis in mice infected aerogenically with *Mycobacterium tuberculosis*, Scand. J. Immunol. 53 (2001) 65–71.
[13] P.S. Amenta, A. Martínez-Hernández, R.L. Trelstad, in: I. Dmajanov, J. Linder (Eds.), Repair and Regeneration, Anderson's Pathology, Mosby, St Louis, 1996, pp. 416–447.
[14] H. Yeager Jr., N. Azumi, C.B. Underhill, Fibrosis: the formation of the granuloma matrix, in: W.N. Rom, S.M. Garay (Eds.), Tuberculosis, Little, Brown and Company, Boston, 1996, pp. 363–370.
[15] J.M. Grange, Immunophysiology and immunopathology of tuberculosis, in: P.D.O. Davies (Ed.), Clinical Tuberculosis, vol. 9, Chapman & Hall, London, 1998, pp. 113–127.
[16] S.B. Lucas, Histopathology, in: P.D.O. Davies (Ed.), Clinical Tuberculosis, vol. 8, Chapman & Hall, London, 1998, pp. 113–127.
[17] P.J. Cardona, S. Gordillo, I. Amat, J. Díaz, J. Lonca, C. Vilaplana, A. Pallares, R. Llatjos, A. Ariza, V. Ausina, Catalase-peroxidase activity has no influence on virulence in a murine model of tuberculosis, Tuberculosis (Edinb) 83 (2003) 351–359.
[18] P.J. Cardona, S. Gordillo, J. Diaz, G. Tapia, I. Amat, A. Pallares, C. Vilaplana, A. Ariza, V. Ausina, Widespread bronchogenic dissemination makes DBA/2 mice more susceptible than C57BL/6 mice to experimental aerosol infection with *Mycobacterium tuberculosis*, Infect. Immun. 71 (2003) 5845–5854.
[19] J.E. Gomez, J.D. McKinney, *M. tuberculosis* persistence, latency, and drug tolerance, Tuberculosis (Edinb) 84 (2004) 29–44.
[20] T. Ulrichs, S.H.E. Kaufmann, Cell-mediated immune response, in: W.N. Rom, S.M. Garay, B.R. Bloom (Eds.), Tuberculosis, Lippincott Williams & Wilkins, Philadelphia, 2004, pp. 251–263.
[21] R. Hernandez-Pando, G.A. Rook, The role of TNF-alpha in T-cell-mediated inflammation depends on the Th1/Th2 cytokine balance, Immunology 82 (1994) 591–595.
[22] C.O. Thoen, Tuberculosis in wild and domestic mammals, in: B.R. Bloom (Ed.), Tuberculosis, Pathogenesis, Protection, and Control, ASM Press, Washington, DC, 1994, pp. 157–164.
[23] S.L. Baldwin, C. D'Souza, A.D. Roberts, B.P. Kelly, A.A. Frank, M.A. Lui, J.B. Ulmer, K. Huygen, D.M. McMurray, I.M. Orme, Evaluation of new vaccines in the mouse and guinea pig model of tuberculosis, Infect. Immun. 66 (1998) 2951–2959.
[24] G.W. Comstock, L.B. Edwards, R.N. Philip, W.A. Winn, A comparison in the United States of America of two tuberculins, PPD-S and RT 23, Bull. World Health Organ. 31 (1964) 161–170.
[25] C.B. Inderlied, C.A. Kemper, L.E. Bermudez, The *Mycobacterium avium* complex, Clin. Microbiol. Rev. 6 (1993) 266–310.
[26] R.J. Wallace Jr., Nontuberculous mycobacterial infections in the human immunodeficiency virus-negative host, in: W.N. Rom, S.M. Garay, B.R. Bloom (Eds.), Tuberculosis, Lippincott Williams & Wilkins, Philadelphia, 2004, pp. 651–662.
[27] W.D. Travis, T.V. Colby, M.N. Koss, M.L. Rosado-de-Christenson, N.L. Müller, T.E. King Jr., Non-neoplastic disorders of the lower respiratory tract, American Registry of Pathology and the Armed Forces Institute of Pathology, Washington, DC, 2002 pp. 539–728.
[28] D.C. Farhi, U.G. Masonh III, C.R. Horsburgh Jr., Pathologic findings in disseminated *Mycobacterium avium-intracellulare* infection, Am. J. Clin. Pathol. 85 (1986) 67–72.
[29] M. Partam, S.M. Garay, *Mycobacterium avium-intracellulare* complex and other nontuberculous mycobacterial infections in human immunodeficiency virus-infected patients, in: W.N. Rom, S.M. Garay, B.R. Bloom (Eds.), Tuberculosis, Lippincott Williams & Wilkins, Philadelphia, 2004, pp. 689–709.
[30] V.M. Lima, V.L. Bonato, K.M. Lima, S.A. Dos Santos, R.R. Dos Santos, E.D. Goncalves, L.H. Faccioli, I.T. Brandao, J.M. Rodrigues-Junior, C.L. Silva, Role of trehalose dimycolate in recruitment of cells and modulation of production of cytokines and NO in tuberculosis, Infect. Immun. 69 (2001) 5305–5312.
[31] R. Ryll, Y. Kumazawa, I. Yano, Immunological properties of trehalose dimycolate (cord factor) and other mycolic acid-containing glycolipids–a review, Microbiol. Immunol. 45 (2001) 801–811.
[32] J. Indrigo, R.L. Hunter Jr., J.K. Actor, Cord factor trehalose 6,6′-dimycolate (TDM) mediates trafficking events during mycobacterial infection of murine macrophages, Microbiology 149 (2003) 2049–2059.
[33] V. Rao, N. Fujiwara, S.A. Porcelli, M.S. Glickman, *Mycobacterium tuberculosis* controls host innate immune activation through cyclopropane modification of a glycolipid effector molecule, J. Exp. Med. 201 (2005) 535–543.
[34] L. Ozmen, M. Pericin, J. Hakimi, R.A. Chizzonite, M. Wysocka, G. Trinchieri, M. Gately, G. Garotta, Interleukin 12, interferon gamma, and tumor necrosis factor alpha are the key cytokines of the generalized Shwartzman reaction, J. Exp. Med. 180 (1994) 907–915.

[35] O.C. Turner, R.J. Basaraba, I.M. Orme, Immunopathogenesis of pulmonary granulomas in the guinea pig after infection with *Mycobacterium tuberculosis*, Infect. Immun. 71 (2003) 864–871.

[36] T.M. Lasco, O.C. Turner, L. Cassone, I. Sugawara, H. Yamada, D.N. McMurray, I.M. Orme, Rapid accumulation of eosinophils in lung lesions in guinea pigs infected with *Mycobacterium tuberculosis*, Infect. Immun. 72 (2004) 147–149.

[37] C.A. Scanga, V.P. Mohan, K. Tanaka, D. Alland, J.L. Flynn, J. Chan, The inducible nitric oxide synthase locus confers protection against aerogenic challenge of both clinical and laboratory strains of *Mycobacterium tuberculosis* in mice, Infect. Immun. 69 (2001) 7711–7717.

[38] A.M. Cooper, L.B. Adams, D.K. Dalton, R. Appelberg, S. Ehlers, IFN-gamma and NO in mycobacterial disease: new jobs for old hands, Trends Microbiol. 10 (2002) 221–226.

[39] R. Guler, M.L. Olleros, D. Vesin, R. Parapanov, C. Vesin, S. Kantengwa, L. Rubbia-Brandt, N. Mensi, A. Angelillo-Scherrer, E. Martinez-Soria, F. Tacchini-Cottier, I. Garcia, Inhibition of inducible nitric oxide synthase protects against liver injury induced by mycobacterial infection and endotoxins, J. Hepatol. 41 (2004) 773–781.

[40] C.D. D'Souza, A.M. Cooper, A.A. Frank, R.J. Mazzaccaro, B.R. Bloom, I.M. Orme, An anti-inflammatory role for gamma delta T lymphocytes in acquired immunity to *Mycobacterium tuberculosis*, J. Immunol. 158 (1997) 1217–1221.

[41] P.J. Murray, R.A. Young, Increased antimycobacterial immunity in interleukin-10-deficient mice, Infect. Immun. 67 (1999) 3087–3095.

[42] I.S. Leal, M. Florido, P. Andersen, R. Appelberg, Interleukin-6 regulates the phenotype of the immune response to a tuberculosis subunit vaccine, Immunology 103 (2001) 375–381.